Electronic Supplementary Material (ESI) for Physical Chemistry Chemical Physics.

Insights into non-thermal plasma chemistry of acetone diluted in N_2/O_2 mixtures: a real-time MS experiment

Sébastien Thomas[a], Nicole Blin-Simiand[b], Michel Héninger[a] , Pascal Jeanney[b], Joel Lemaire[a] , Lionel Magne[b] , Hélène Mestdagh[a], Stéphane Pasquiers[b], Essyllt Louarn[*a,c†]

a- Université Paris-Saclay, CNRS, Institut de Chimie Physique, UMR8000, 91405 Orsay, France

b- Université Paris-Saclay, CNRS, Laboratoire de Physique des Gaz et des Plasma, UMR8578, 91405 Orsay, France

c- Université Claude Bernard Lyon 1, CNRS, Institut de Recherche sur la Catalyse et l'Environnement de Lyon, UMR5256, 69626 Villeurbanne, FRANCE

TABLE OF CONTENTS

Table S1. Kinetic reactions cited in the text are summarized in this table. Index represent the reaction number in the text. Rate coefficient k of the reactions are at 298 K or otherwise stated. Kinetic data are taken from NIST kinetic database[1] when available, from plasma chemistry published reactivity, or from JPL database[2] otherwise. The order of the reaction is generally bimolecular (noted 2) or termolecular (noted 3). In that case reaction rates are calculated for a pressure of 0.46 bar.

Index	**Reaction**	**rate k ($cm^3\ s^{-1}$ or $cm^6\ s^{-1}$)**	**ord.**	**Ref.**
Plasma initial reactions				
3	$N_2^* + O_2 \rightarrow 2\,O + N_2$	Function of the nitrogen excited state [2×10^{-12} to 3×10^{-10}]	2	3,4
	$O(^1D) + N_2 \rightarrow O(^3P) + N_2$	2.6×10^{-11}	2	3
	$O(^1D) + O_2 \rightarrow O(^3P) + O_2$	4.0×10^{-11}	2	2
6	$N_2^* + O \rightarrow NO + N$	7.0×10^{-12}	2	3,4
7	$N + O \rightarrow NO$	1.02×10^{-32}	3	3,4
8	$O + O_2 \rightarrow O_3$	6.1×10^{-34}	3	2–4
	$O + NO \rightarrow NO_2$	9.1×10^{-32}	3	2
26	$H + O \rightarrow OH$	7.7×10^{-31}	3	5
S18	$H + O_2 \rightarrow HO_2$	5.3×10^{-32}	3	2
VOC degradation reactions				
9	$N_2^* + CH_3COCH_3 \rightarrow$ products	~5.5×10^{-11}	2	6,7
9a	$N_2^* + CH_3COCH_3 \rightarrow CH_3^{\bullet} + CH_3CO^{\bullet} + N_2$ †		2	
9b	$N_2^* + CH_3COCH_3 \rightarrow H^{\bullet} + {}^{\bullet}CH_2COCH_3 + N_2$		2	
22	$N_2^* + HCN \rightarrow H + CN + N_2$	4.4×10^{-12}	2	7
23	$N_2^* + CH_3CN \rightarrow$ products		2	7
23a	$N_2^* + CH_3CN \rightarrow CH_3 + CN + N_2$	3.9×10^{-12}	2	
23b	$N_2^* + CH_3CN \rightarrow H + CH_2CN$	9.1×10^{-12}	2	
27	$N_2^* + CH_2O \rightarrow$ products $+ N_2$	5.0×10^{-10}	2	6
S25	$N_2^* + CH_2O \rightarrow H + HCO + N_2$	2.5×10^{-10}		
35	$N_2^* + CH_2CO \rightarrow$ products $+ N_2$	6.5×10^{-10}	2	7
36	$N_2^* + CH_3CHO \rightarrow$ products $+ N_2$	4.2×10^{-11}	2	8
11	$O + CH_3COCH_3 \rightarrow CH_3COCH_2 + OH$ *	7.5×10^{-16}	2	1,9

---

[*] Predominant reaction pathway

	$O + HCN \rightarrow$ products $O + HCN \rightarrow NCO + H$	1.5×10^{-17}	2	2
	$O + CH_3CN \rightarrow$ products	3.1×10^{-15} [321 K]	2	10
	$O + C_2H_5CN \rightarrow$ products	1.0×10^{-14} [354 K]	2	10
4	$O + C_2H_6 \rightarrow OH + C_2H_5$	3.9×10^{-18}	2	1
 S26	$O + CH_2O \rightarrow$ products $O + CH_2O \rightarrow OH + HCO$	1.6×10^{-13}	2	2
 33/S28 S2	$O + CH_2CO \rightarrow$ products $O + CH_2CO \rightarrow HCO + HCO$ $O + CH_2CO \rightarrow CH_2O + CO$	3.8×10^{-13}	2	1
33	$O + CH_3CHO \rightarrow OH + CH_3CO$	4.5×10^{-13}	2	2
	$O + HONO \rightarrow OH + NO_2$	9.1×10^{-16}	2	11
	$OH + CH_3COCH_3 \rightarrow$ products $OH + CH_3COCH_3 \rightarrow CH_3COCH_2 + H_2O$ †	2.2×10^{-13}	2	1 2
	$OH + HCN \rightarrow$ products	3.1×10^{-14}	2	2
	$OH + CH_3CN \rightarrow$ products	2.3×10^{-14}	2	2
	$OH + C_2H_5CN \rightarrow$ products	1.8×10^{-14}	2	12
5	$OH + C_2H_6 \rightarrow H_2O + C_2H_5$	2.5×10^{-13}	2	1,2
S27	$OH + CH_2O \rightarrow H_2O + HCO$ †	1.0×10^{-11}	2	1
	$OH + CH_3OH \rightarrow$ products	9.1×10^{-13}	2	2
 34/S4/S29	$OH + CH_2CO \rightarrow$ products $OH + CH_2CO \rightarrow HCO + CH_2O$ $OH + CH_2CO \rightarrow CO + CH_2OH$	1.7×10^{-11} 50% 50%	2	1
34	$OH + CH_3CHO \rightarrow H_2O + CH_3CO$	1.6×10^{-11} †	2	1,2
	$OH + CH_3ONO_2 \rightarrow$ products	2.8×10^{-14}	2	2
Intermediate reactions				
21	$N + CH2 \rightarrow CN + H_2$	1.6×10^{-11}	2	14–16
 12a 12b	$N + CH_3 \rightarrow$ products $N + CH_3 \rightarrow HCN + H_2$ $N + CH_3 \rightarrow H_2CN + H$ †	9.5×10^{-11}	2	1,17,18
 18	$N + C_2H_3 \rightarrow$ products $N + C_2H_3 \rightarrow CH_3CN$ $N + C_2H_3 \rightarrow C_2H_2 + NH$	7.7×10^{-11} 4% 16%	2	19
13	$N + H_2CN \rightarrow HCN + NH$	~5×10^{-11}	2	1
17	$N + HCO \rightarrow HCN + O$	5.8×10^{-12}	2	

---

† predominant reaction pathway with a yield of 93±18%[13]

14	$H + H_2CN \rightarrow HCN + H_2$	5×10^{-10}	2	17,18
	$H + CH_3CO \rightarrow$ products	5.5×10^{-11}	2	1
16/S24	$H + CH_3CO \rightarrow CH_3 + HCO$	65%		
29	$H + CH_3CO \rightarrow CH_2CO + H_2$	35%		
S9	$H + CH_3O_2 \rightarrow OH + CH_3O$	1.6×10^{-10}	2	1
S1	$O + CH_3 \rightarrow CH_2O + H\ ^{\dagger}$	1.4×10^{-10}	2	1
30/S3	$O + CH_3CO \rightarrow CH_2CO + OH$	6.4×10^{-11}	2	
S11	$O + CH_3O_2 \rightarrow CH_3O + O_2$	6.0×10^{-11}	2	1
S5	$O_2 + CH_3 \rightarrow CH_3O_2$	4.3×10^{-31}	3	1,2
47	$O_2 + CN \rightarrow NCO + O$	2.4×10^{-11}	2	1,20
	$O_2 + HCO \rightarrow CO + HO_2$	5.2×10^{-12}	2	2
S7	$O_2 + CH_3CO \rightarrow CH_3C(O)O_2$	5.0×10^{-12}	2	1
48	$OH + CN \rightarrow NCO + H^{\cdot}$	7.0×10^{-11}	2	1
25/S19	$OH + CH_3 \rightarrow CH_3OH$	$9{,}5\times10^{-30}$	3	1
39	$OH + NO \rightarrow HONO$	7.1×10^{-32}	3	2
S20	$OH + CH_3O_2 \rightarrow CH_3OH + O_2$	1×10^{-10}	2	1
40	$HO_2 + NO \rightarrow HNO_3$	1.5×10^{-31}	3	
S17	$HO_2 + CH_3O \rightarrow CH_2O + H_2O_2$	5.0×10^{-13}	2	1
S21	$HO_2 + CH_3O \rightarrow CH_3OH + O_2$	1.8×10^{-11}	2	1
44	$NO + CH_3 \rightarrow CH_3NO$	4.0×10^{-11}	3	1
42	$NO + CH_3O \rightarrow CH_3ONO$	2.3×10^{-29}	3	1,2
43	$NO + CH_2{=}C(O)CH_3 \rightarrow C_3H_5ONO$	3.1×10^{-11}	2	21
41a	$NO_2 + CH_3 \rightarrow CH_3NO_2$	3.4×10^{-11}	3	1
41b	$NO_2 + CH_3 \rightarrow CH_3ONO$	$\sim10^{-13}$	3	1
	$NO_2 + CH_3 \rightarrow CH_3O + NO$	2.3×10^{-11}	2	22
	$NO_2 + CH_3O \rightarrow CH_2O + HONO$	2.0×10^{-13}	2	2
45	$NO_2 + CH_3O \rightarrow CH_3ONO_2$	5.5×10^{-29}	3	1,2
19	$CN + CH_3CN \rightarrow HCN + CH_2CN$	1.2×10^{-12}	2	1
15	$H_2CN + H_2CN \rightarrow HCN + CH_2NH$	3.85×10^{-12}	2	1
20	$CH_3 + CH_2CN \rightarrow C_2H_5CN$	unknown	2	15
	$CH_3 + NCO \rightarrow$ products	$(2.1 \pm 0.8)\times10^{-10}$	2	23
46	$CH_3 + NCO \rightarrow CH_3NCO\ ^{\dagger}$	Dominant		
	$CH_3 + HCO \rightarrow$ products	2.3×10^{-10}	2	1
31	$CH_3 + HCO \rightarrow CH_3CHO$	13%		
	$CH_3 + HCO \rightarrow CH_4 + CO$	12%		
S14	$CH_3 + CH_3O \rightarrow CH_2O + CH_4$	4.0×10^{-11}	2	1

S10	$CH_3 + CH_3O_2 \rightarrow CH_3O + CH_3O$	4.0×10^{-11}	2	1
38	$CH_3 + COOCH_3 \rightarrow CH_3C(O)OCH_3$	5.0×10^{-11}	2	24
45	$HCO + NCO \rightarrow HNCO + CO$	6.0×10^{-11}	2	1
24	$HCO + HCO \rightarrow CH_2O + CO$	5.0×10^{-11}	2	1
S22	$HCO + CH_3O \rightarrow CH_3OH + CO$	1.5×10^{-10}		1
32	$HCO + CH_3CO \rightarrow CO + CH_3CHO$	1.5×10^{-11}		1
37	$CH_2OH + CH_3CO \rightarrow CH_3C(O)CH_2OH$			25
S15	$CH_3O + CH_3O \rightarrow CH_2O + CH_3OH$	1.0×10^{-10}		1
28a/S16 28b/S23	$CH_3O + CH_3CO \rightarrow CH_2O + CH_3CHO$ $CH_3O + CH_3CO \rightarrow CH_3OH + CH_2CO$	1.0×10^{-11} 1.0×10^{-11}		1 1
S6 S12	$CH_3O_2 + CH_3O_2 \rightarrow CH_2O + CH_3OH + O_2$ $CH_3O_2 + CH_3O_2 \rightarrow CH_3O + CH_3O + O_2$	1.25×10^{-13} 1.25×10^{-13}		1 1
S13	$CH_3O_2 + CH_3CO \rightarrow CH_3 + CH_3O + CO_2$	4.0×10^{-11}		1
S8	$CH_3O_2 + CH_3C(O)O_2 \rightarrow$ products $CH_3O_2 + CH_3C(O)O_2 \rightarrow CH_2O + CH_3COOH + O_2$ $CH_3O_2 + CH_3C(O)O_2 \rightarrow CH_3O + CH_3CO_2 + O_2$	1.8×10^{-12} 50%		1

Table S2. Kinetic parameters of proton transfer from H_3O^+ used for the identified molecules. Polarizability (in 10^{-24} cm^3), dipole moment (in D) and proton affinity (PA) (in kJ mol^{-1}) are from NIST database[26]. The kinetic rate coefficient k_M is obtained from the literature (see last column for references) and is given in 10^{-9} cm^3 s^{-1}. The capture rate coefficient k_C is calculated knowing the polarizability and the dipole moment according to Su and Chesnavich[27]. Branching ratios are obtained from the references or otherwise stated.

Name	**Formula**	**Polarisability$^{\#}$**	**Dipole moment**	**PA**	**Ions**	**branching ratio**	**k_M [k_C]**	**Ref k_M**
acetone	C_3H_6O	6.270	2.88	812	$C_3H_7O^+$	100%	3.9[3.9]	28,29
hydrogen cyanide	HCN	2.593	2.98	713	CH_2N^+	100%	3.5[4.2]	30,31
acetonitrile	CH_3CN	4.280	3.92	779	$C_2H_4N^+$	100%	4.9[5.1]	30,31
methanol	CH_3OH	3.210	1.7	754	CH_5O^+	100%	2.7[2.7]	32
formaldehyde	CH_2O	2.770	2.33	713	CH_3O^+	100%	3.4[3.4]	29,33
acetaldehyde	C_2H_4O	4.278	2.69	768	$C_2H_5O^+$	100%	3.6[3.7]	28,29
ketene	C_2H_2O	4.4	1.42	825	$C_2H_3O^+$	100%	2.0[2.4]	33
nitrous acid	HONO				**$H_2NO_2^+$** **NO^+**	**63% *** **37%**	[2.6]	34,35
methyl nitrite	CH_3ONO	4.51	2.05	799			[2.9]	
nitromethane	CH_3NO_2	4.80	3.46[36]	755	$CH_4NO_2^+$	100%	4.1 [4.4]	33
nitric acid	HNO_3			751	$H_2NO_3^+$	100%	1.6 [2.4]	37
methyl nitrate	CH_3ONO_2	5.5	3.081		**$CH_4NO_3^+$** **CH_3OH^+**	**76% *** **24%**	[3.9]	
Isocyanic acid	HNCO	3.2	2.16[38]	753	CH_2NO^+	100%	[2.9]	

methyl isocyanate	CH_3NCO	4.97	3.03[38]	764	$C_2H_4NO^+$	100%	[3.9]	

calculated from Miller and Savchik[39]

* from this study

Table S3. List of observed ions (except precursor ions and isotopes) after 620 discharges for 500 ppm of acetone in a N_2/O_2 mix with various oxygen content. Species present all for at least one oxygen content concentration above 0.05%.

Ion	**Neutral species**	**exact mass of the ion (Da)**	**measured mass (Da)***	**delta mass δm (mDa)**	**relative signal (in %) for different O_2 amount**				
					0%	**1%**	**2%**	**3%**	**5%**
$CHN.H^+$	HCN	28.0182	28.0241	5.9	**6.08**	2.94	2.09	1.45	1.00
NO^+	fragment HONO	29.9980	30.0030	5.0	n.d.#	0.24	0.34	0.38	**0.45**
$CH_2O.H^+$	CH_2O	31.0178	31.0228	5.0	0.11	1.12	1.46	**1.75**	1.69
$CH_4O.H^+$	CH_3OH	33.0335	33.0399	6.4	0.05	**0.19**	0.18	0.17	0.13
$C_3H_4.H^+$	fragment C_3H_6 or C_3H_4	41.0386	41.0422	3.6	0.01	0.08	0.09	0.10	**0.11**
$C_2H_3N.H^+$	H_3CCN	42.0338	42.0400	6.2	**1.10**	0.64	0.50	0.37	0.27
$C_2H_2O.H^+$	CH_2CO	43.0178	43.0211	3.3	0.02	0.09	0.11	**0.12**	**0.12**
$CHNO.H^+$	HNCO	44.0131	44.0169	3.8	0.04	**0.17**	0.14	0.12	0.08
$C_2H_4O.H^+$	CH_2CHO	45.0335	45.0372	3.7	0.07	**0.13**	**0.13**	**0.13**	0.12
$CH_2O_2.H^+$	HCOOH	47.0128	47.0154	2.6	0.02	0.05	**0.06**	**0.06**	**0.06**
$HNO_2.H^+$	HONO	48.0080	48.0101	2.1	0.01	0.35	0.53	0.60	**0.72**
$C_3H_5N.H^+$	CH_3CH_2CN	56.0495	56.0515	2.0	**0.17**	0.10	0.08	0.07	0.04
$C_2H_3NO.H^+$	CH_2CHNO	58.0287	58.0273	-1.4	0.04	**0.06**	0.05	0.04	0.02
$C_3H_6O.H^+$	acetone	59.0491	59.0491	0.0	3.09	11.46	13.75	16.69	**17.55**
$CH_3NO_2.H^+$	CH_3NO_2	62.0237	62.0208	-2.8	0.02	0.24	0.27	**0.30**	**0.30**

$CH_3NO_3.H^+$	CH_3ONO_2	78.0186	78.0069	-11.7	0.01	0.04	0.05	0.06	**0.07**
$C_3H_5NO_2.H^+$	$C_3H_5NO_2$	88.0393	88.0188	-20.5	n.d.	0.03	0.05	0.07	**0.09**

* the measured mass is taken for the experiment which presents the highest amount.

[#] not detected

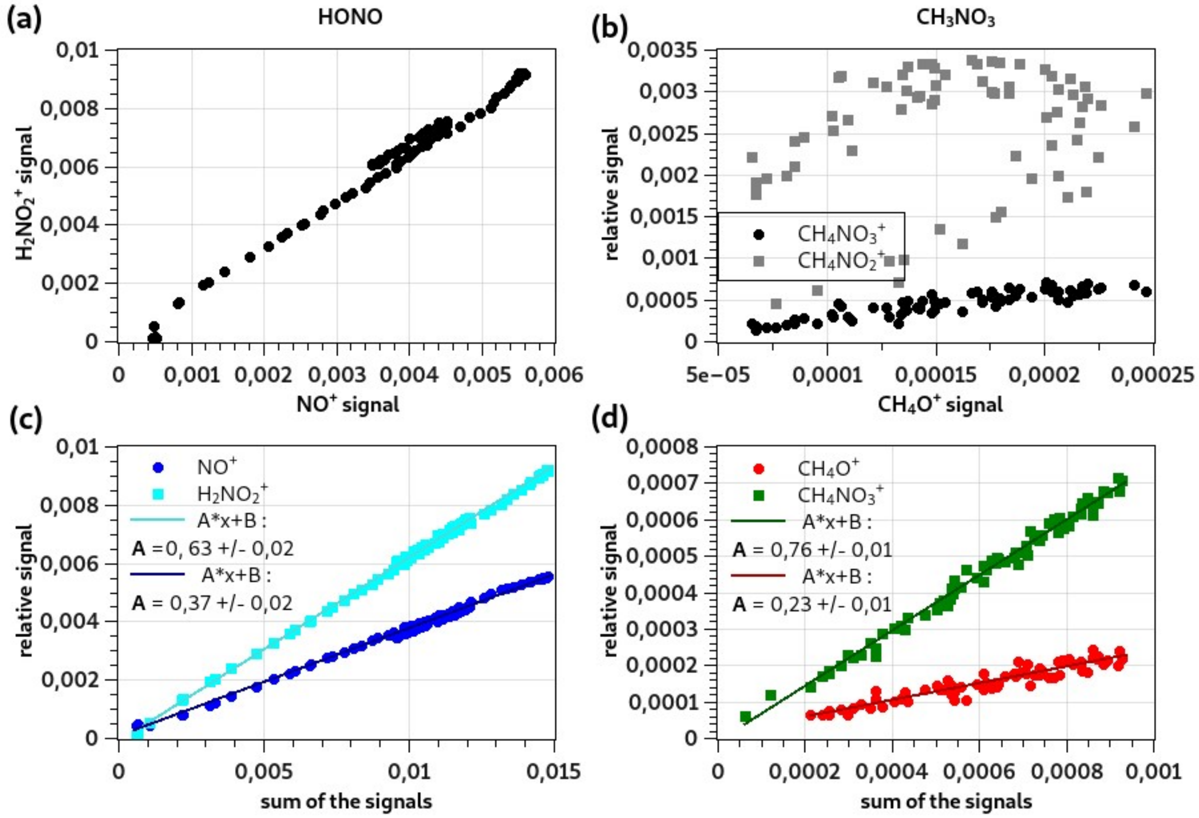

Figure S1. Ion fragments for HONO (a and c) and CH_3NO_3 (b and d) protonation. The signals are taken from experiments at 3% and 5% oxygen so that height precision is correct.

Above: comparison of the relative ion signal for ion fragments (a) $H_2NO_2^+$ versus NO^+ for HONO and (b) $CH_4NO_3^+$ and $CH_4NO_2^+$ versus CH_4O^+ for CH_3NO_3. Linearity of the signals over all discharge numbers is characteristic of ions arising from a fragmentation of the same species. In (b), $CH_4NO_2^+$ and CH_4O^+ are then not related by a direct fragmentation process.

Below: branching ratio for (c) HONO protonation and (d) from CH_3NO_3 protonation calculated from comparison of sum of the signal of fragment ions towards signal of fragment ions.

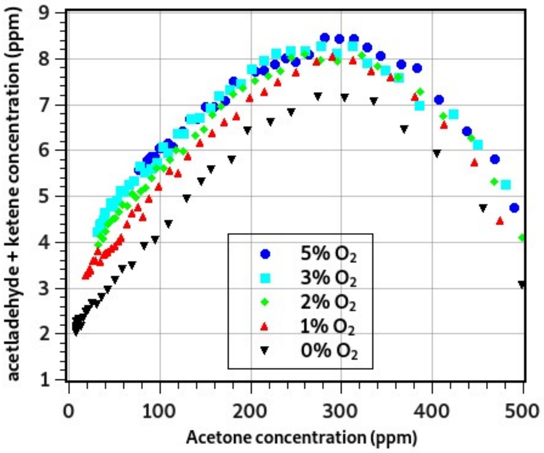

Figure S2. Evolution of the averaged concentrations of the sum of ketene and acetaldehyde compared to acetone concentration.

Ketene and acetaldehyde are supposed to be due to the same radical precursor CH_3CO. The behavior of the combined ketene+acetaldehyde is equivalent whatever oxygen concentration and only depends on acetone concentration.

Annex 1. Main kinetic processes involved in the production of formaldehyde (CH_2O) and methanol (CH_3OH), specific to mixtures containing oxygen, are described here, based on the exiting literature[1]. See also reactions (19)-(24) in the main text.

Kinetic processes for the production of formaldehyde

The main direct reaction for the production of CH_2O is:

$$O + CH_3 \rightarrow CH_2O + H \quad \text{(S1)}$$

But several indirect paths should be also considered:

$$O + CH_2CO \rightarrow CH_2O + CO \quad \text{(S2)}$$

$$O + CH_3CO \rightarrow OH + CH_2CO \quad \text{(S3)}$$

which is a source of the hydroxyl radical, followed by:

$$OH + CH_2CO \rightarrow HCO + CH_2O \quad \text{(S4)}$$

Most importantly at atmospheric pressure, the methyl group add to oxygen to form the methyl peroxyl:

$$O_2 + CH_3 + N_2 \rightarrow CH_3O_2 + N_2 \quad \text{(S5)}$$

followed by:

$$CH_3O_2 + CH_3O_2 \rightarrow CH_2O + CH_3OH + O_2 \quad \text{(S6)}$$

Also important is the formation of the radical $CH_3C(O)O_2$:

$$O_2 + CH_3CO + N_2 \rightarrow CH_3C(O)O_2 + N_2 \quad \text{(S7)}$$

followed by:

$$CH_3O_2 + CH_3C(O)O_2 \rightarrow CH_2O + CH_3COOH + O_2 \quad \text{(S8)}$$

Other routes concern the methoxy radical, CH_3O, produced by several reactions:

$$H + CH_3O_2 \rightarrow OH + CH_3O \quad \text{(S9)}$$

$$CH_3 + CH_3O_2 \rightarrow CH_3O + CH_3O \quad \text{(S10)}$$

$O + CH_3O_2 \rightarrow CH_3O + O_2$ (S11)

$CH_3O_2 + CH_3O_2 \rightarrow CH_3O + CH_3O + O_2$ (S12)

$CH_3O_2 + CH_3CO \rightarrow CH_3 + CH_3O + CO_2$ (S13)

which is followed by:

$CH_3 + CH_3O \rightarrow CH_2O + CH_4$ (S14)

$CH_3O + CH_3O \rightarrow CH_2O + CH_3OH$ (S15)

$CH_3O + CH_3CO \rightarrow CH_2O + CH_3CHO$ (S16)

$HO_2 + CH_3O \rightarrow CH_2O + H_2O_2$ (S17)

where the hydroperoxyl radical is readily produced by the three-body process:

$H + O_2 + N_2 \rightarrow HO_2 + N_2$ (S18)

Kinetic processes for the production of methanol

Methanol is coming from (S6) and (S15), and more directly:

$OH + CH_3 + N_2 \rightarrow CH_3OH + N_2$ (S19)

In addition, the following reactions should be considered:

$OH + CH_3O_2 \rightarrow CH_3OH + O_2$ (S20)

$HO_2 + CH_3O \rightarrow CH_3OH + O_2$ (S21)

$HCO + CH_3O \rightarrow CH_3OH + CO$ (S22)

$CH_3O + CH_3CO \rightarrow CH_3OH + CH_2CO$ (S23)

where the HCO radical can come from various reactions:

$H + CH_3CO \rightarrow CH_3 + HCO$ (S24)

$N_2^* + CH_2O \rightarrow H + HCO + N_2$ (S25)

$O + CH_2O \rightarrow OH + HCO$ (S26)

$OH + CH_2O \rightarrow H_2O + HCO$ (S27)

$$O + CH_2CO \rightarrow HCO + HCO \tag{S28}$$

$$OH + CH_2CO \rightarrow HCO + CH_2O \tag{S29}$$

REFERENCES

(1) Manion, J. A.; Huie, R. E.; Levin, R. D.; Jr, D. R. B.; Orkin, V. L.; Tsang, W.; McGivern, W. S.; Hudgens, J. W.; Knyazev, V. D.; Atkinson, D. B.; Chai, E.; Tereza, A. M.; Lin, C.-Y.; T. C. Allison and, W. G. M.; Westley, F.; Herron, J. T.; Hampson, R. F.; D. H. Frizzell. NIST Chemical Kinetics Database. NIST Standard Reference Database 17, Version 7.0 (Web Version), Release 1.6.8, 2015.

(2) Burkholder, J. B.; Sander, S. P.; Abbatt, J.; Barker, J. R.; Cappa, C.; Crounse, J. D.; Dibble, T. S.; Huie, R. E.; Kolb, C. E.; Kurylo, M. J.; Orkin, V. L.; Percival, C. J.; Wilmouth, D. M.; Wine, P. H. Chemical Kinetics and Photochemical Data for Use in Atmospheric Studies, Evaluation No. 19. *Jet Propulsion Laboratory, Pasadena* **2019**, *19* (5), 1610.

(3) Kossyi, I. A.; Kostinsky, A. Y.; Matveyev, A. A.; Silakov, V. P. Kinetic Scheme of the Non-Equilibrium Discharge in Nitrogen-Oxygen Mixtures. *Plasma Sources Sci. Technol.* **1992**, *1* (3), 207–220. https://doi.org/10.1088/0963-0252/1/3/011.

(4) Guerra, V.; Tejero-del-Caz, A.; Pintassilgo, C. D.; Alves, L. L. Modelling N2–O2 Plasmas: Volume and Surface Kinetics. *Plasma Sources Sci. Technol.* **2019**, *28* (7), 073001. https://doi.org/10.1088/1361-6595/ab252c.

(5) Magne, L.; Pasquiers, S.; Blin-Simiand, N.; Postel, C. Production and Reactivity of the Hydroxyl Radical in Homogeneous High Pressure Plasmas of Atmospheric Gases Containing Traces of Light Olefins. *J. Phys. D: Appl. Phys.* **2007**, *40* (10), 3112–3127. https://doi.org/10.1088/0022-3727/40/10/015.

(6) Pasquiers, S.; Blin-Simiand, N.; Magne, L. Dissociation against Oxidation Kinetics for the Conversion of VOCs in Non-Thermal Plasmas of Atmospheric Gases. *Eur. Phys. J. Appl. Phys.* **2016**, *75* (2), 24703. https://doi.org/10.1051/epjap/2016150575.

(7) Herron, J. T. Evaluated Chemical Kinetics Data for Reactions of N(2D), N(2P), and N2(A3Σu+) in the Gas Phase. *Journal of Physical and Chemical Reference Data* **1999**, *28* (5), 1453–1483. https://doi.org/10.1063/1.556043.

(8) Faider, W.; Pasquiers, S.; Blin-Simiand, N.; Magne, L. Effect of Oxygen on the Conversion of Acetaldehyde in Homogeneous Plasmas of N2/O2/CH3CHO Mixtures. *Plasma Sources Sci. Technol.* **2013**, *22* (6), 065010. https://doi.org/10.1088/0963-0252/22/6/065010.

(9) Hou, H.; Li, Y.; Wang, B. Computational Study of the Reaction of Atomic Oxygen with Acetone in the Gas Phase. *J. Phys. Chem. A* **2006**, *110* (49), 13163–13171. https://doi.org/10.1021/jp065346w.

(10) Budge, S.; Roscoe, J. M. The Reactions of O(3P) with Acetonitrile and Propionitrile. *Can. J. Chem.* **1995**, *73* (5), 666–674. https://doi.org/10.1139/v95-085.

(11) Tsang, W.; Herron, J. T. Chemical Kinetic Data Base for Propellant Combustion I. Reactions Involving NO, NO2, HNO, HNO2, HCN and N2O. *Journal of Physical and Chemical Reference Data* **1991**, *20* (4), 609–663. https://doi.org/10.1063/1.555890.

(12) Harris, G. W.; Kleindienst, T. E.; Pitts, J. N. Rate Constants for the Reaction of OH Radicals with CH3CN, C2H5CN AND CH2□CH-CN in the Temperature Range 298–424 K. *Chemical Physics Letters* **1981**, *80* (3), 479–483. https://doi.org/10.1016/0009-2614(81)85061-0.

(13) Cameron, M.; Sivakumaran, V.; Dillon, T. J.; Crowley, J. N. Reaction between OH and CH3CHO. *Phys. Chem. Chem. Phys.* **2002**, *4* (15), 3628–3638. https://doi.org/10.1039/B202586H.

(14) Moreau, N.; Pasquiers, S.; Blin-Simiand, N.; Magne, L.; Jorand, F.; Postel, C.; Vacher, J.-R. Propane Dissociation in a Non-Thermal High-Pressure Nitrogen Plasma. *J. Phys. D: Appl. Phys.* **2010**, *43* (28), 285201. https://doi.org/10.1088/0022-3727/43/28/285201.

(15) Koeta, O.; Blin-Simiand, N.; Faider, W.; Pasquiers, S.; Bary, A.; Jorand, F. Decomposition of Acetaldehyde in Atmospheric Pressure Filamentary Nitrogen Plasma. *Plasma Chem Plasma Process* **2012**, *32* (5), 991–1023. https://doi.org/10.1007/s11090-012-9388-6.

(16) Tsai, C. Ping.; McFadden, D. L. Gas-Phase Atom-Radical Kinetics of Atomic Hydrogen, Nitrogen, and Oxygen Reactions with Fluoromethylene Radicals. *J. Phys. Chem.* **1990**, *94* (8), 3298–3300. https://doi.org/10.1021/j100371a017.

(17) Marston, G.; Nesbitt, F. L.; Stief, L. J. Branching Ratios in the N+CH3 Reaction: Formation of the Methylene Amidogen (H2CN) Radical. *J. Chem. Phys.* **1989**, *91* (6), 3483–3491. https://doi.org/10.1063/1.456878.

(18) Cimas, A.; Largo, A. The Reaction of Nitrogen Atoms with Methyl Radicals: Are Spin-Forbidden Channels Important? *J. Phys. Chem. A* **2006**, *110* (37), 10912–10920. https://doi.org/10.1021/jp0634959.

(19) Payne, W. A.; Monks, P. S.; Nesbitt, F. L.; Stief, L. J. The Reaction between N(4S) and C2H3: Rate Constant and Primary Reaction Channels. *J. Chem. Phys.* **1996**, *104* (24), 9808–9815. https://doi.org/10.1063/1.471740.

(20) Baulch, D. L.; Cobos, C. J.; Cox, R. A.; Frank, P.; Hayman, G.; Just, Th.; Kerr, J. A.; Murrells, T.; Pilling, M. J.; Troe, J.; Walker, R. W.; Warnatz, J. Evaluated Kinetic Data for Combustion Modeling. Supplement I. *Journal of Physical and Chemical Reference Data* **1994**, *23* (6), 847–848. https://doi.org/10.1063/1.555953.

(21) Delbos, E.; Devolder, P.; ElMaimouni, L.; Fittschen, C.; Brudnik, K.; Jodkowski, J. T.; Ratajczak, E. Pressure and Temperature Dependence of the Rate Constants for the Association Reactions of Vinoxy and 1-Methylvinoxy Radicals with Nitric Oxide. *Phys. Chem. Chem. Phys.* **2002**, *4* (13), 2941–2949. https://doi.org/10.1039/B110100E.

(22) Srinivasan, N. K.; Su, M.-C.; Sutherland, J. W.; Michael, J. V. Reflected Shock Tube Studies of High-Temperature Rate Constants for OH + CH4 → CH3 + H2O and CH3 + NO2 → CH3O + NO. *J. Phys. Chem. A* **2005**, *109* (9), 1857–1863. https://doi.org/10.1021/jp040679j.

(23) Gao, Y.; Macdonald, R. G. Determination of the Rate Constant for the Radical−Radical Reaction NCO(X2Π) + CH3(X2A2‘ ‘) at 293 K and an Estimate of Possible Product Channels. *J. Phys. Chem. A* **2006**, *110* (3), 977–989. https://doi.org/10.1021/jp058247b.

(24) Hassinen, E.; Riepponen, P.; Blomqvist, K.; Kalliorinne, K.; Evseev, A. M.; Koskikallio, J. Kinetics of Reactions between Methoxycarbonyl, Methyl, and Methoxy Radicals Formed in Flash Photolysis of Dimethyl Oxalate in Gas Phase. *International Journal of Chemical Kinetics* **1985**, *17* (10), 1125–1134. https://doi.org/10.1002/kin.550171009.

(25) Tsang, W. Chemical Kinetic Data Base for Combustion Chemistry. Part 2. Methanol. *Journal of Physical and Chemical Reference Data* **1987**, *16* (3), 471–508. https://doi.org/10.1063/1.555802.

(26) Lias, S. G.; Bartmess, J. E.; Liebman, J. F.; Holmes, J. L.; Levin, R. D.; Mallard, W. G. Ion Energetics Data. In *NIST Chemistry WebBook*; Lindstrom, P. J., Mallard, W. G., Eds.; NIST Standard Reference Database Number 69; Gaithersburg MD.

(27) Su, T.; Chesnavich, W. J. Parametrization of the Ion–Polar Molecule Collision Rate Constant by Trajectory Calculations. *J. Chem. Phys.* **1982**, *76* (10), 5183–5185. https://doi.org/10.1063/1.442828.

(28) Lindinger, W.; Hansel, A.; Jordan, A. On-Line Monitoring of Volatile Organic Compounds at Pptv Levels by Means of Proton-Transfer-Reaction Mass Spectrometry (PTR-MS) Medical Applications, Food Control and Environmental Research. *International Journal of Mass Spectrometry and Ion Processes* **1998**, *173* (3), 191–241. https://doi.org/10.1016/S0168-1176(97)00281-4.

(29) Spanel, P.; Ji, Y.; Smith, D. SIFT Studies of the Reactions of H3O+, NO+ and O2+ with a Series of Aldehydes and Ketones. *Int. J. Mass Spectrom. Ion Proc.* **1997**, *165–166*, 25–37. https://doi.org/10.1016/S0168-1176(97)00166-3.

(30) Mackay, G. I.; Betowski, L. D.; Payzant, J. D.; Schiff, H. I.; Bohme, D. K. Rate Constants at 297.Degree.K for Proton-Transfer Reactions with Hydrocyanic Acid and Acetonitrile. Comparisons with Classical Theories and Exothermicity. *J. Phys. Chem.* **1976**, *80* (26), 2919–2922. https://doi.org/10.1021/j100567a019.

(31) Tanaka, K.; Mackay, G. I.; Bohme, D. K. Rate and Equilibrium Constant Measurements for Gas-Phase Proton-Transfer Reactions Involving H2O, H2S, HCN, and H2CO. *Can. J. Chem.* **1978**, *56* (2), 193–204. https://doi.org/10.1139/v78-031.

(32) Spanel, P.; Smith, D. SIFT Studies of the Reactions of H3O+, NO+ and O2+ with a Series of Alcohols. *Int. J. Mass Spectrom. Ion Proc.* **1997**, *167–168*, 375–388. https://doi.org/10.1016/S0168-1176(97)00085-2.

(33) Mackay, G. I.; Tanner, S. D.; Hopkinson, A. C.; Bohme, D. K. Gas-Phase Proton-Transfer Reactions of the Hydronium Ion at 298 K. *Can. J. Chem.* **1979**, *57* (12), 1518–1523. https://doi.org/10.1139/v79-248.

(34) Lee, A.; Goldstein, A. H.; Kroll, J. H.; Ng, N. L.; Varutbangkul, V.; Flagan, R. C.; Seinfeld, J. H. Gas-Phase Products and Secondary Aerosol Yields from the Photooxidation of 16 Different Terpenes. *Journal of Geophysical Research: Atmospheres* **2006**, *111* (D17). https://doi.org/10.1029/2006JD007050.

(35) Metzger, A.; Dommen, J.; Gaeggeler, K.; Duplissy, J.; Prevot, A. S. H.; Kleffmann, J.; Elshorbany, Y.; Wisthaler, A.; Baltensperger, U. Evaluation of 1,3,5 Trimethylbenzene Degradation in the Detailed Tropospheric Chemistry Mechanism, MCMv3.1, Using Environmental Chamber Data. *Atmospheric Chemistry and Physics* **2008**, *8* (21), 6453–6468. https://doi.org/10.5194/acp-8-6453-2008.

(36) Dey, A.; Fernando, R.; Abeysekera, C.; Homayoon, Z.; Bowman, J. M.; Suits, A. G. Photodissociation Dynamics of Nitromethane and Methyl Nitrite by Infrared Multiphoton Dissociation Imaging with Quasiclassical Trajectory Calculations: Signatures of the Roaming Pathway. *J. Chem. Phys.* **2014**, *140* (5), 054305. https://doi.org/10.1063/1.4862691.

(37) Fehsenfeld, F. C.; Howard, C. J.; Schmeltekopf, A. L. Gas Phase Ion Chemistry of HNO3. *J. Chem. Phys.* **1975**, *63* (7), 2835–2841. https://doi.org/10.1063/1.431722.

(38) Ivanova, E. V.; Muchall, H. M. Hydrolysis of N-Sulfinylamines and Isocyanates: A Computational Comparison. *J. Phys. Chem. A* **2007**, *111* (42), 10824–10833. https://doi.org/10.1021/jp075210d.

(39) Miller, K. J.; Savchik, J. A New Empirical Method to Calculate Average Molecular Polarizabilities. *J. Am. Chem. Soc.* **1979**, *101* (24), 7206–7213. https://doi.org/10.1021/ja00518a014.